

# Mechanism of Ozone Decomposition on a Manganese Oxide Catalyst.

## 2. Steady-State and Transient Kinetic Studies

Wei Li<sup>†</sup> and S. Ted Oyama<sup>\*,\*‡</sup>

Contribution from the Departments of Chemical Engineering and Chemistry, Virginia Polytechnic Institute and State University, Blacksburg, Virginia 24061-0211

Received April 27, 1998

**Abstract:** This paper presents an in-depth study of the mechanism of ozone decomposition on a manganese oxide catalyst as studied by in situ Raman spectroscopy and kinetic measurements. In the companion paper, the reaction intermediate was identified to be a peroxide species by using isotopic substitution and ab initio calculations. To ascertain the role of the intermediate in the catalytic reaction, we investigated its steady-state and transient kinetics, as well as the steady-state kinetics of the overall decomposition reaction, at temperatures from 281 to 340 K and ozone partial pressures from 4.7 Pa to 2.1 kPa. The steady-state and transient kinetics were found to be well-represented by a two-step sequence consisting of (i) adsorption of ozone to form the peroxide species, and (ii) desorption of molecular oxygen. The surface was found to be nonuniform, with activation energies that varied linearly with amount of surface coverage. At zero surface coverage the activation energy for ozone adsorption was 6.2 kJ mol<sup>-1</sup>; that for molecular oxygen desorption was 69.0 kJ mol<sup>-1</sup>. The steady-state surface coverages derived from the transient results are in excellent agreement with those measured at steady-state conditions, and the transient desorption kinetics are well-described by the kinetic parameters obtained from the steady-state data, indicating that the proposed reaction sequence accurately describes the mechanism of decomposition.

### Introduction

This paper reports a study of the mechanism of ozone decomposition on manganese oxide, one of the most active transition metal oxides for this reaction. The work includes determination of the steady-state and transient kinetics, measurement of the surface coverage during reaction by use of in situ Raman spectroscopy, and analysis of the results by use of uniform and nonuniform surface kinetic treatments.

Observation and identification of adsorbed species under reaction conditions are essential steps in establishing reaction mechanisms. However, not all observed species necessarily play an important role in the catalytic cycle.<sup>1</sup> In fact, in some cases the most abundant species on the catalyst surfaces are merely passive spectators that do not participate in the reaction.<sup>2</sup> To ascertain the role of an adsorbed species in a catalytic cycle, its steady-state and transient kinetic behaviors have to be determined and shown to be consistent with the overall kinetics of the reaction.<sup>1</sup>

As reported in the companion paper,<sup>3</sup> an adsorbed species was observed on a manganese oxide catalyst during the ozone decomposition reaction and was identified as a peroxide species by using in situ Raman spectroscopy measurements with isotopic substitution experiments, combined with ab initio molecular

orbital calculations. The objective of this paper is to investigate the steady-state and transient kinetics of this species to determine its role in the ozone decomposition reaction.

It is commonly believed that the relationship between kinetic data and mechanism model is unidirectional,<sup>4</sup> in the sense that a mechanism can be used to derive a rate expression, but kinetic data alone cannot be used to establish a mechanism. Usually more than one model can give a reasonably good fit to kinetic data. However, transient adsorption and desorption measurements in combination with surface coverage information can provide the additional information needed to pinpoint a reaction mechanism.<sup>1</sup> Using the techniques discussed here, we will show that the ozone decomposition reaction proceeds by two kinetically significant steps: the adsorption of ozone to form a peroxide intermediate, and the decomposition of this intermediate to produce molecular oxygen.

### Experimental Section

Details of the experimental setup have been presented previously.<sup>3</sup> Briefly, the kinetic measurements were carried out on a 10 wt % MnO<sub>2</sub>/Al<sub>2</sub>O<sub>3</sub> sample prepared by the incipient wetness impregnation method. Its surface area, measured by the Brunauer–Emmett–Teller method, was 87 m<sup>2</sup> g<sup>-1</sup>. The sample (0.20 g) was pressed into a wafer 1 mm thick and 15 mm in diameter, and was kept spinning at 1000 rpm to avoid sample overheating. Prior to all measurements the samples were pretreated in flowing oxygen at 773 K for 3 h. Ozone was produced by passing filtered oxygen (Airco, >99.6%) through a high-voltage silent-discharge ozone generator (OREC, V5-0). The mixture of ozone

(3) Li, W.; Oyama, S. T.; Gibbs, G. V. *J. Am. Chem. Soc.* **1998**, *120*, 9041.

(4) (a) Dumesic, J. A.; Rudd, D. F.; Aparicio, L. M.; Rekoske, J. E.; Trevino, A. A. *The Microkinetics of Heterogeneous Catalysis*; American Chemical Society: Washington, DC, 1993; p 24. (b) Burwell, R. L. *Catalysis: Sci., Technol.* **1991**, *9*, 1–85.

\* To whom correspondence should be addressed.

<sup>†</sup> Department of Chemical Engineering.

<sup>‡</sup> Departments of Chemical Engineering and Chemistry.

(1) Tamaru, K. *Dynamic Heterogeneous Catalysis*; Academic Press: London, 1978.

(2) (a) Noto, Y.; Fukuda, K.; Onishi, T.; Tamaru, K. *Trans. Faraday Soc.* **1967**, *63*, 2300. (b) Ekerdt, J. G.; Bell, A. T. *J. Catal.* **1978**, *48*, 111. (c) Yamasaki, H.; Kobori, Y.; Naito, S.; Onishi, T.; Tamaru, K. *J. Chem. Soc., Faraday Trans. 1* **1981**, *77*, 2913. (d) Galuszka, J.; Chang, J. R.; Amenomiya, Y. *Proc. 7th Int. Congr. Catal.* **1981**, 529. (e) Zhang, W.; Oyama, S. T. *J. Am. Chem. Soc.* **1996**, *118*, 7173–7177.

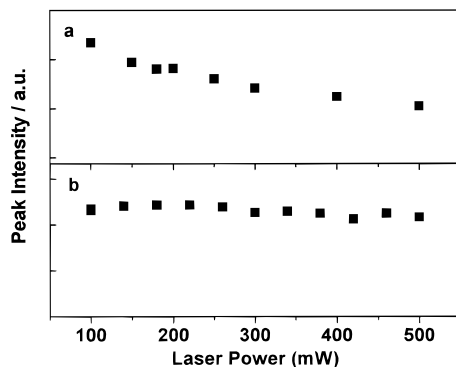


**Figure 1.** Effects of laser power and sample spin rate on the Raman signal intensity of the observed peroxide species. Room temperature ( $\sim 298$  K), 2 mol % ozone in oxygen ( $1000 \text{ cm}^3 \text{ min}^{-1}$ ), slit width =  $50 \mu\text{m}$  (resolution =  $\sim 6 \text{ cm}^{-1}$ ). (a) sample spin rate = 800 rpm; (b) sample spin rate = 1000 rpm.

and oxygen with a controlled partial pressure of ozone could be introduced into an in situ Raman cell at various temperatures. The volume of the cell was small ( $<25 \text{ cm}^3$ ), permitting rapid ( $<1.5$  s) gas-phase changes in transient experiments. An UV absorption-type ozone analyzer (IN-USA, AFX-H1) was used to measure the concentrations of ozone. The reaction temperature was varied from 281 to 340 K, the total pressure was 101 kPa, and the ozone partial pressure was changed from 4.7 Pa to 2.1 kPa. The flow rate of the ozone/oxygen mixture was set at  $744 \mu\text{mol s}^{-1}$  ( $1000 \text{ cm}^3 \text{ min}^{-1}$ ). The steady-state rate was determined by monitoring ozone concentrations at the inlet and outlet of the Raman cell, and the turnover rate was calculated by using an active center concentration of  $160 \mu\text{mol}$ , based on an estimate of the dispersion of the catalyst from X-ray diffraction ( $\sim 70\%$ ). Conversion ranged from 8 to 23% in the conditions of this study. Turnover rates are calculated from the conversion data by the expression,  $\text{rate} = (\text{conversion} \times \text{flow rate} \times \text{ozone concentration}) / \text{number of sites}$ .

## Results

**Effect of Laser.** To investigate the behavior of the peroxide species quantitatively, one must make sure that the laser beam will not influence the concentration or the reaction kinetics of the species. By comparing the ozone decomposition activity at conditions with and without the laser on, we found that the laser did not affect the decomposition rate under the reaction conditions used here. This probably results from the high flow rate of the ozone/oxygen mixture and the fast spin rate of the sample. We also investigated the effect of laser power on the coverage of the peroxide species (i.e., Raman signal intensity). Raman spectra of the adsorbed species were acquired at different laser powers, while the total detector exposure ( $\propto$  laser power  $\times$  exposure time) was fixed by adjusting the exposure time. When the sample was spun at 800 rpm, the peak intensity dropped gradually with increasing laser power (Figure 1a). As will be seen, the peak intensity is directly related to the coverage. This indicates that, under this condition, the laser radiation caused a decrease in the concentration of the surface species, probably through local heating of the sample. However, when the spin rate was increased to 1000 rpm (Figure 1b), the peak area stayed constant with increasing laser power. Hence at this spin rate, the effect of the laser on the surface species was negligible. All the kinetic data reported hereafter were obtained by using the latter spin rate.

**Steady-State Kinetics.** The effects of reaction temperature and ozone partial pressure on the decomposition rate and surface coverage of the peroxide species were examined under steady-state conditions. The steady-state rate was found to increase with increasing ozone partial pressure and increasing temper-

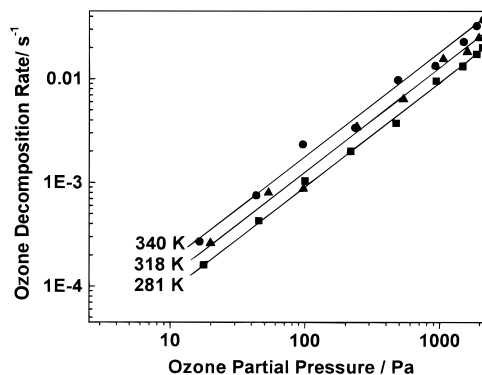


**Figure 2.** Effects of temperature and ozone partial pressure on ozone decomposition rate. Reactant flow rate =  $1000 \text{ cm}^3 \text{ min}^{-1}$ .

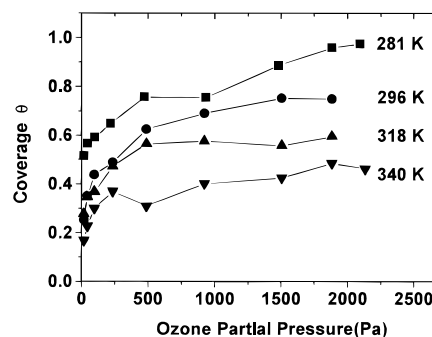


**Figure 3.** Reaction isotherms of the ozone decomposition reaction measured by using in situ Raman spectroscopy. Reactant flow rate =  $1000 \text{ cm}^3 \text{ min}^{-1}$ . Spectral acquisition conditions: laser power = 100 mW, resolution =  $6 \text{ cm}^{-1}$ , exposure = 30 s, and 60 scans.

ature (Figure 2), as expected. The reaction order on ozone partial pressure was found to be slightly  $<1$  (0.94), independent of temperature. Previous work had found that the reaction rate did not depend on oxygen partial pressure.<sup>5</sup>

The surface coverage,  $\theta$ , of the peroxide intermediate under reaction conditions was determined by integrating the peak intensity of the signal at  $884 \text{ cm}^{-1}$  in the Raman spectra and normalizing to the peak intensity at the lowest temperatures and highest ozone pressures, where saturation occurred. The surface coverage was determined at various reaction conditions and plotted as reaction isotherms (Figure 3). As expected for an adsorbed species, its surface coverage increased with increasing ozone partial pressure and decreased with increasing temperature. The Clausius–Clapeyron plot of the coverage data can be obtained by taking horizontal slices at fixed values for surface coverage of the peroxide intermediate (Figure 4). The slopes of the lines yield the differential or isosteric heat of reaction.

$$\Delta H = R \left( \frac{d \ln P}{d(1/T)} \right)_{\theta} \quad (1)$$

The isosteric heat of reaction was found to decrease with coverage (Figure 5):

$$\Delta H (\text{kJ mol}^{-1}) = -22 - 89\theta \quad (2)$$

**Transient Kinetics.** To gather further information on the kinetic behavior of the adsorbed peroxide species, we carried out transient experiments to study the adsorption and decomposition of this species separately. The transient adsorption experiments were initiated with a bare surface having no adsorbed peroxide species. Ozone was introduced suddenly and the Raman spectra were acquired at successive time intervals

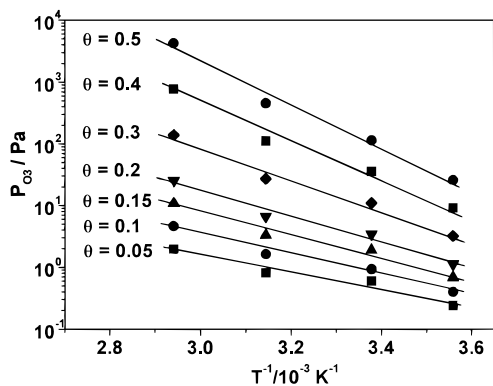


**Figure 4.** Clausius–Clapeyron plots of the coverage data obtained by taking horizontal slices at fixed values for surface coverage of the peroxide intermediate.

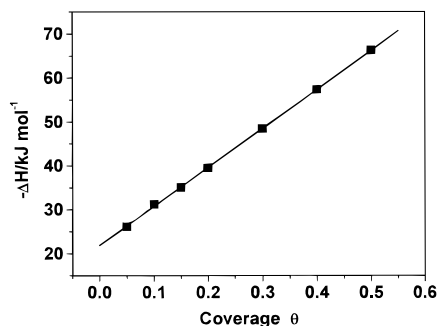


**Figure 5.** Effect of surface coverage on the isosteric heat of reaction obtained from the slope of the Clausius–Clapeyron plots.

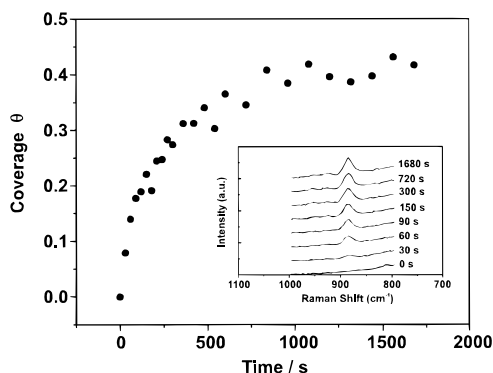


**Figure 6.** Typical set of Raman signals for a transient adsorption experiment (inset) and the corresponding adsorption curve. Reactant flow rate = 1000 cm<sup>3</sup> min<sup>-1</sup>, response time < 3 s. Ozone partial pressure = 100 Pa and temperature = 296 K. Laser power = 100 mW, resolution = 6 cm<sup>-1</sup>, exposure = 20 s.

(~30 s). The peak areas were integrated, and the coverages were calculated and plotted versus the elapsed time. Figure 6 presents a typical set of Raman signals for a transient adsorption experiment (inset) and the corresponding adsorption curve. Figure 7 shows the adsorption curves at various temperatures and ozone partial pressures. As expected, the adsorption process is faster at higher ozone partial pressures (Figure 7, bottom), and the final coverage is also higher for higher ozone partial pressures, in agreement with the steady-state results.

The transient desorption experiments were carried out similarly to the adsorption measurements, except that the starting surface was preadsorbed with the peroxide species and the ozone was suddenly removed from the gas stream. Figure 8 shows the coverage versus time curves during desorption experiments at various temperatures. Again, as expected, the desorption process is faster at higher temperatures.

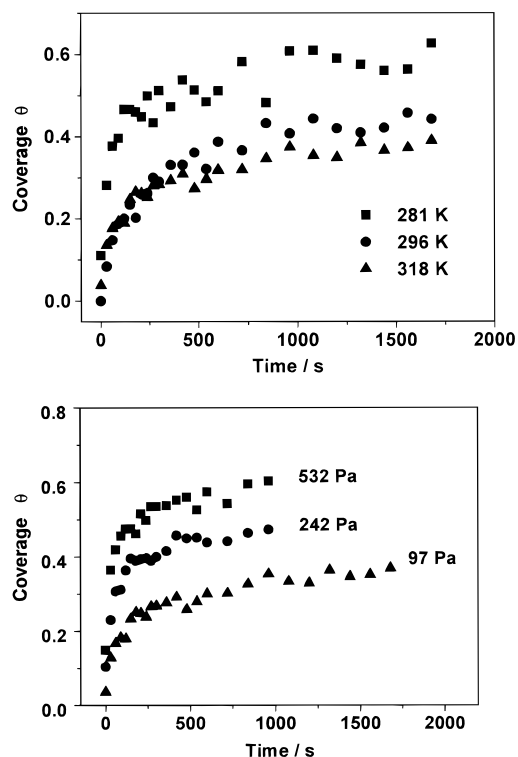


**Figure 7.** (Top) Effect of temperature on the transient adsorption curve. Reactant flow rate = 1000 cm<sup>3</sup> min<sup>-1</sup>, response time < 3 s. Ozone partial pressure = 120 Pa; spectral acquisition conditions are the same as in Figure 6. (Bottom) Effect of ozone partial pressure on the transient adsorption curve. Temperature = 318 K; spectral acquisition conditions are as in Figure 6.

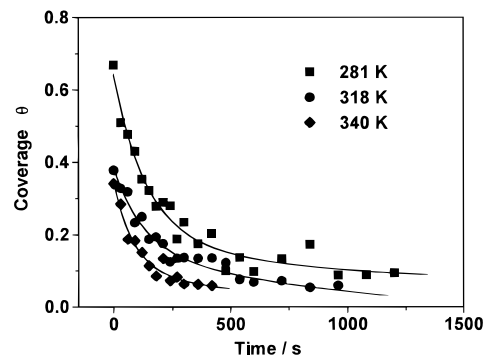


**Figure 8.** Effect of temperature on the transient desorption curve. Reactant flow rate = 1000 cm<sup>3</sup> min<sup>-1</sup>, response time < 3 s. Spectral acquisition conditions are the same as in Figure 6. The solid lines are fitted curves using  $\theta = -h^{-1} \ln[hk_d^0(t - t_0)]$ .

## Discussion

**Steady-State Kinetics.** In the first paper of this pair,<sup>3</sup> we proposed a reaction sequence (Scheme 1) consisting of (i) dissociative adsorption of ozone to form an oxygen molecule and an atomic oxygen species, (ii) ozone reaction with an atomic oxygen species to form a peroxide species and an oxygen molecule, and (iii) decomposition of the peroxide species to produce molecular oxygen. All steps are taken to be irreversible. Evidence that the first and second steps are irreversible is the absence of observed ozone in any desorption experiments or in separate temperature-programmed desorption experiments after ozone adsorption, only molecular oxygen being detected by mass spectrometry.<sup>6</sup> Proof that the second step is irreversible is the

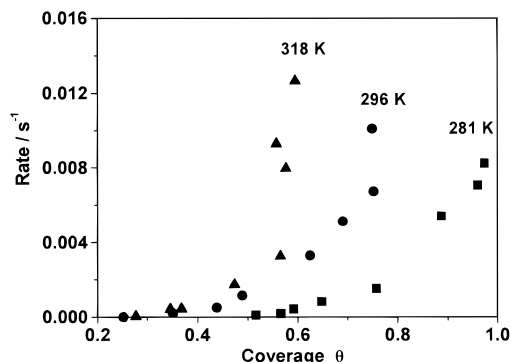


**Figure 9.** Plots of reaction rate vs surface coverage. A linear relationship is expected for the uniform surface model.

observations that there was no effect of oxygen partial pressure on the rate of decomposition<sup>5</sup> and that the peroxide species was not detected when oxygen alone was present in the gas phase. If the adsorption of oxygen to form the peroxide intermediate were possible, then increasing its partial pressure would have increased the surface coverage and retarded the rate of adsorption of ozone, and consequently the rate of the overall reaction. This was not observed, and both steps can be considered to be substantially irreversible from a kinetic standpoint. We recognize, of course, that no elementary step is completely irreversible.

#### Scheme 1. Proposed Ozone Decomposition Mechanism



Since step (i) by itself is much faster than steps (ii) and (iii), and does not involve the most-abundant reaction intermediate, the peroxide species, the reaction mechanism can be reduced to a two-step sequence, in which only the second and third steps are kinetically meaningful. Also, since the catalyst surface is quickly covered by the atomic oxygen species once it is brought into contact with ozone, step (ii) can also be viewed as ozone adsorption onto an atomic oxygen-covered surface site. To check this two-step sequence against the kinetic results, we used both uniform and nonuniform surface models to fit the steady-state decomposition data.

**Uniform Surface Kinetic Analysis.** If the surface of the catalyst were uniform, the reaction rate for ozone decomposition would have been given by  $r = k_d\theta$ , and would have been expected to be proportional to the surface coverage ( $\theta$ ) of the peroxide species. However, this is clearly not the case because the rate is highly nonlinear in coverage (Figure 9). Also the isosteric heat of reaction obtained from the Clausius–Clapeyron plot of the coverage data increases with coverage (Figure 5), indicating that a nonuniform surface treatment should be utilized.

**Nonuniform Surface Kinetic Analysis.** A nonuniform surface is a surface that has catalytic sites of different affinities for the reactant, the products, or both.<sup>7</sup> The classic case of a nonuniform surface is that of an Fe catalyst for ammonia

**Table 1.** Kinetic Parameters of the Nonuniform Surface Model

$$g = 0.75 \quad h = 11.8$$

$$k_a^0, \text{ cm}^3 \text{ s}^{-1} = 3.1 \times 10^{-18} \exp\left(-\frac{6.2 \text{ kJ mol}^{-1}}{RT}\right)$$

$$k_d^0, \text{ s}^{-1} = 1.6 \times 10^7 \exp\left(-\frac{69.0 \text{ kJ mol}^{-1}}{RT}\right)$$

synthesis.<sup>8</sup> Details of the derivation of nonuniform surface kinetics can be found elsewhere.<sup>9</sup> In summary, for a surface with an activation energy for adsorption that increases linearly with coverage, i.e.,  $E_a = E_a^0 + gRT\theta$ , the adsorption rate can be shown to be  $r_a = k_a^0(\text{O}_3)e^{-g\theta}$ , which is the Elovich equation.<sup>10</sup> Here  $k_a^0$  is the adsorption rate constant at zero coverage, and  $g$  is the proportionality constant for linear dependence of activation energy with coverage. Similarly, if the activation energy for desorption decreases linearly with coverage ( $E_d = E_d^0 - hRT\theta$ ), the desorption rate can be expressed as:  $r_d = k_d^0e^{h\theta}$ , where  $k_d^0$  is the desorption rate constant at zero coverage, and  $h$  is the proportionality constant for linear dependence of desorption activation energy with coverage; this is the Langmuir equation, first derived for desorption from tungsten filaments.<sup>9</sup> At steady state, the rate is  $r_{ss} = r_a = r_d$ , from which the steady-state coverage can be obtained. The rate,  $r_{ss}$ , is then derived by substituting the coverage into either of the two rate equations. In summary, this yields the following formulation of the steady-state coverage and rate determined for a nonuniform surface model:

$$\theta_{ss} = \frac{1}{g+h} \ln \left[ \frac{k_a^0(\text{O}_3)}{k_d^0} \right] \quad (3)$$

$$r_{ss} = k_d^0 \left[ \frac{k_a^0}{k_d^0} (\text{O}_3) \right]^{h/(g+h)} \quad (4)$$

From these expressions it follows that the steady-state coverage should depend linearly on the logarithm of the ozone partial pressure, whereas the decomposition rate should depend on a fractional power of the ozone partial pressure,  $h/(g+h) < 1$ . The experimental data were found to be well-described by these expressions (Figures 2 and 10). We also confirmed that the exponent in the power rate law expression did not vary significantly with temperature (Figure 2). In addition, the decomposition rate increased only slowly with temperature, because of the small apparent activation energy for this reaction. The values of the parameters in the rate expression (Table 1) were obtained by carrying out a least-squares fitting of the steady-state surface coverage and rate data with eqs 3 and 4 and using  $k_a^0 = A_a^0 \exp(-E_a^0/RT)$  and  $k_d^0 = A_d^0 \exp(-E_d^0/RT)$ . Note that the proportionality constant for linear dependence of adsorption activation energy with coverage,  $g$ , was very small (0.75) compared with that for desorption,  $h$  (11.8). This indicates that the activation energy for adsorption does not change significantly with coverage, whereas the activation energy for desorption is strongly dependent on the surface coverage. Meanwhile, the activation energy at zero coverage  $E_a^0$  was calculated to be 6.2 kJ mol<sup>-1</sup>, which suggests that

(8) Brunauer, S.; Love, K. S.; Keenan, R. G. *J. Am. Chem. Soc.* **1942**, *64*, 751.

(9) (a) Langmuir, *J. Am. Chem. Soc.* **1932**, *54*, 2798–2832. (b) Kubokawa, Y. *Bull. Chem. Soc. Jpn.* **1960**, *33*, 734–738. (c) Kubokawa, Y. *Bull. Chem. Soc. Jpn.* **1960**, *33*, 1226–1228. (d) Boudart, M.; Egawa, C.; Oyama, S. T.; Tamaru, K. *J. Chim. Phys.* **1981**, *78*, 987.

(10) Aharoni, C.; Tomkins, F. C. *Adv. Catal.* **1970**, *21*, 1–49.

(6) Li, W.; Oyama, S. T. Unpublished results.

(7) Boudart, M.; Djega-Mariadassou, G. *Kinetics of Heterogeneous Catalytic Reactions*; Princeton University Press: Princeton, NJ, 1984.

ozone adsorption on the catalyst surface is essentially not activated and is consistent with the strong oxidizing nature of ozone. On the other hand, desorption of molecular oxygen was found to have an activation energy  $E_d^0$  of  $69.0 \text{ kJ mol}^{-1}$  at zero coverage, and this activation energy decreased considerably with increasing coverage. The obtained preexponential factor for adsorption  $A_a^0$  ( $3.1 \times 10^{-18} \text{ cm}^3 \text{ s}^{-1}$ ) was consistent with the values predicted by transition state theory<sup>11</sup> ( $10^{-10}$ – $10^{-17} \text{ cm}^3 \text{ s}^{-1}$ ). However, the obtained preexponential factor for desorption  $A_d^0$  ( $1.6 \times 10^7 \text{ s}^{-1}$ ) was significantly smaller than the predicted values ( $10^{13}$ – $10^{17} \text{ s}^{-1}$ ). Expressing the preexponential factor as  $A = (kT/h) \exp(\Delta S^\ddagger/R)$ , we calculated the value of  $\Delta S^\ddagger_d$  to be  $-107 \text{ J mol}^{-1} \text{ K}^{-1}$ . The loss of entropy indicates that some degrees of freedom present in the reactants have been lost at the transition state. The calculated entropy change is in good agreement with the estimated value for two-dimensional translational motion of the peroxide species on the surface ( $104 \text{ J mol}^{-1} \text{ K}^{-1}$ ). It is possible that the adsorbed peroxide intermediate has free lateral two-dimensional translational motion but loses it at the transition state, which must have motion perpendicular to the surface.

To understand the origin of the nonuniformity of the surface, one should consider the uniqueness of manganese oxides. Manganese exists in several stable oxidation states (+2, +3, +4, +7).<sup>12</sup> A recent study of  $\text{Al}_2\text{O}_3$ -supported manganese oxide using electron spin resonance and diffuse reflectance spectroscopy<sup>13</sup> reported that the manganese species were present as a mixture of  $\text{Mn}^{2+}$ ,  $\text{Mn}^{3+}$ , and  $\text{Mn}^{4+}$ . Our observation of  $\text{Mn}_3\text{O}_4$  by Raman spectroscopy<sup>3</sup> confirms that on the catalyst surface the manganese consists of mixed valence compounds of  $\text{Mn}^{2+}$  and  $\text{Mn}^{3+}$ . Hence, not only may the surface structure of the manganese oxides be different, but also the manganese species in various oxidation states can be expected to have different affinities to ozone, resulting in a kinetically or thermodynamically nonuniform surface. In addition, lateral interactions between the adsorbates can also exert an influence at high coverages.

**Transient Kinetics.** To unambiguously identify a surface species as a reaction intermediate rather than a passive spectator, it is essential to carry out dynamic measurements of the species and relate its kinetic behavior to the overall kinetics.

The adsorption and desorption rates can be obtained by differentiating the adsorption and desorption curves, respectively (Figures 7 and 8). This method was first utilized to describe ammonia decomposition on a tungsten foil.<sup>14</sup> An example of such a procedure is given at 318 K (Figure 11). For the desorption curves (since there is no re-adsorption), the rate of desorption is given directly from the slope of the plot of  $\theta$  vs  $t$ ,  $r_d = -d\theta/dt$ . However, for the adsorption curves, the slope gives the net adsorption rate,  $d\theta/dt = r_a - r_d$ , since  $\text{O}_2$  is desorbing at the same time as adsorption is occurring. The absolute rate of adsorption,  $r_a$ , is then given by the slope of the adsorption plot plus the value of the desorption rate,  $r_a = d\theta/dt + r_d$ . The latter is measured separately as just described, and is taken at the same value of coverage as the adsorption rate. These equations allow independent calculation of the rates of the two elementary steps. The results are shown in Figure

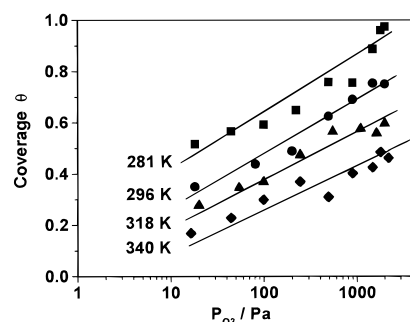


**Figure 10.** Plots for the surface coverage vs the logarithm of ozone partial pressure. A linear relationship is expected for the nonuniform surface case.

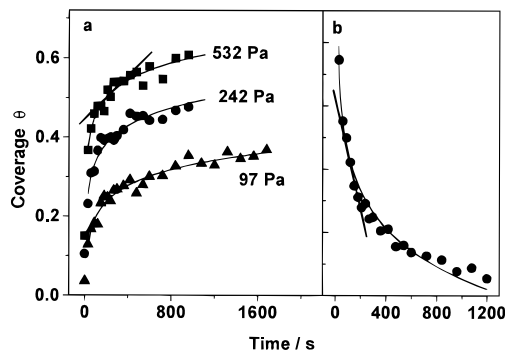


**Figure 11.** Transient results: (a) adsorption curves; (b) desorption curves.  $T = 318 \text{ K}$ , reactant flow rate =  $1000 \text{ cm}^3 \text{ min}^{-1}$ , response time  $< 3 \text{ s}$ . Spectrum acquisition conditions: laser power =  $100 \text{ mW}$ , resolution =  $6 \text{ cm}^{-1}$ , exposure =  $20 \text{ s}$ . The adsorption and desorption rates can be calculated from the slopes of the curves, as shown.

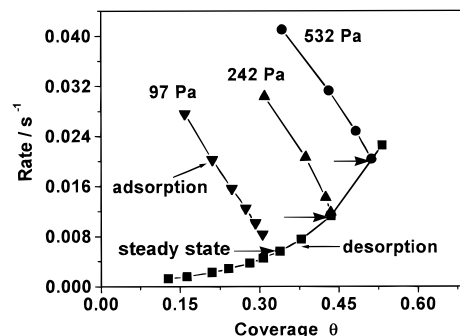


**Figure 12.** Transient adsorption and desorption rates vs surface coverage. Conditions as in Figure 11. The desorption rate (squares) is independent of the pressure and increases with surface coverage. The adsorption curves are the three data sets (circles, up triangles, and down triangles) that decrease with coverage and rise to higher values as the pressure increases. The intersections of the curves correspond to the steady-state coverages.

12. The adsorption curves are the three data sets that decrease with coverage, which (as expected) attain higher values with increasing pressure. The desorption points, on the other hand, do not depend on pressure and increase with coverage.

At steady state the rate of adsorption equals the rate of desorption, and the steady-state points can be obtained at the intersection of the adsorption and desorption curves (Figure 12). The so-obtained steady-state coverages at 318 K were compared with those measured in the steady-state experiments (Table 2), and excellent agreement was obtained. This result demonstrates that the transient kinetic data are consistent with the steady-state data and are in support of the proposed reaction sequence.

A further confirmation can be obtained if the kinetic parameters obtained from the steady-state results (Table 1) can

(11) (a) van Santen, R. A.; Niemantsverdriet, J. W. *Chemical Kinetics and Catalysis*; Plenum: New York, 1995. (b) Zhdanov, V. P.; Pavlicek, J.; Knor, Z. *Catal. Rev.-Sci. Eng.* **1989**, *30*, 501.

(12) Cotton, F. A.; Wilkinson, G. *Advanced Inorganic Chemistry*, 5th ed.; Wiley: New York, 1988.

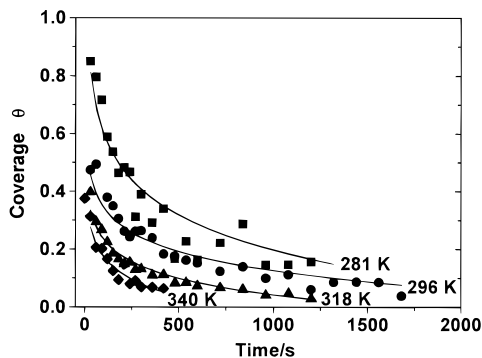
(13) Kijlstra, W. S.; Poels, E. K.; Bliëk, A.; Weckhuysen, B. M.; Schoonheydt, R. A. *J. Phys. Chem. B* **1997**, *101*, 309.

(14) Shindo, H.; Egawa, C.; Onishi, T.; Tamaru, K. *J. Chem. Soc., Faraday Trans. 1* **1980**, *76*, 280.

**Table 2.** Comparison of the Steady-State Coverage Obtained from Transient and Steady-State Experiments:  $T = 318\text{ K}$ 

	O <sub>3</sub> pressure, Pa					
	97		242		532	
	TR*	SS	TR	SS	TR	SS
steady-state coverage	0.34	0.35	0.45	0.44	0.56	0.58

\*Methods: TR = transient, SS = steady state.

**Figure 13.** Comparison of measured transient desorption curves (symbols) with the curves calculated from the steady-state kinetic parameters (solid lines).

be used to predict the transient kinetics. This can be done for the desorption curves, whose rate expression can be integrated analytically. For the desorption data in the transient curves, the rate of desorption is given directly from the slope of the plot of  $\theta$  vs  $t$ ,  $r_d = -d\theta/dt$ . Since  $r_d = k_d^0 e^h \theta$ , by integration we obtain

$$\theta = -\frac{1}{h} \ln[hk_d^0(t - t^0)] \quad (5)$$

where  $t_0 = (hk_d^0 e^{h\theta_0})^{-1}$ , and  $\theta_0$  is the initial coverage. So the transient desorption curve can be calculated by using the values of  $h$  and  $k_d^0$  in Table 1, and the results (solid lines) are plotted in Figure 13 along with the measured curves (symbols). Clearly, the transient desorption kinetics are well-described by the kinetic

parameters obtained from the steady-state results. Because the transient and steady-state data were measured in separate experiments, they serve as independent checks for the validity of the proposed reaction sequence.

In summary, the measured kinetics of the ozone decomposition reaction were found to depend on the partial pressure of ozone to a fractional power. This was exactly as predicted by the rate expression based on two steps, the adsorption of ozone and the desorption of molecular oxygen. The measured rate constants were found to be physically realistic and accurately predicted the coverage during reaction as well as the transient behavior of the catalyst.

## Conclusions

The steady-state and transient kinetics of the ozone decomposition reaction were investigated at temperatures from 281 to 340 K and ozone partial pressures from 4.7 Pa to 2.1 kPa. The reaction proceeds through two kinetically significant, irreversible steps, the adsorption of ozone on the catalyst surface and the desorption of molecular oxygen. The steady-state kinetics were found to be well-described by a nonuniform surface treatment. Ozone adsorption had a low activation energy,  $6.2\text{ kJ mol}^{-1}$ , whereas the desorption of molecular oxygen had an activation energy of  $69.0\text{ kJ mol}^{-1}$  at zero surface coverage. The overall rate of the reaction is given by a balance between the rates of adsorption of ozone and desorption of molecular oxygen. Transient adsorption and desorption experiments, in combination with steady-state kinetic measurements, confirm the role of peroxide species as a reaction intermediate in the ozone decomposition reaction. The measured transient desorption kinetics are in good agreement with those calculated from the steady-state results, indicating that the proposed steps accurately describe the reaction sequence.

**Acknowledgment.** We gratefully acknowledge the financial support for this work by the Director, Division of Chemical and Thermal Systems of the National Science Foundation, under Grant CTS-9712047. We thank Joseph Merola for valuable comments on the reaction mechanism.

JA9814422